



Since January 2020 Elsevier has created a COVID-19 resource centre with free information in English and Mandarin on the novel coronavirus COVID-19. The COVID-19 resource centre is hosted on Elsevier Connect, the company's public news and information website.

Elsevier hereby grants permission to make all its COVID-19-related research that is available on the COVID-19 resource centre - including this research content - immediately available in PubMed Central and other publicly funded repositories, such as the WHO COVID database with rights for unrestricted research re-use and analyses in any form or by any means with acknowledgement of the original source. These permissions are granted for free by Elsevier for as long as the COVID-19 resource centre remains active.



Prognostic value of CT integrated with clinical and laboratory data during the first peak of the COVID-19 pandemic in Northern Italy: A nomogram to predict unfavorable outcome

Enzo Angeli^a, Serena Dalto^b, Stefano Marchese^a, Lucia Setti^c, Manuela Bonacina^c, Francesca Galli^d, Eliana Rulli^d, Valter Torri^d, Cinzia Monti^a, Roberta Meroni^a, Giordano Domenico Beretta^b, Massimo Castoldi^e, Emilio Bombardieri^{e,*}

^a Department of Radiology, Humanitas Gavazzeni, Via Gavazzeni, 21, 24125, Bergamo, BG, Italy

^b Department of Oncology, Humanitas Gavazzeni, Via Gavazzeni, 21, 24125, Bergamo, BG, Italy

^c Department of Nuclear Medicine, Humanitas Gavazzeni, Via Gavazzeni, 21, 24125, Bergamo, BG, Italy

^d Laboratory of Methodology for Clinical Research, Istituto di Ricerche Farmacologiche Mario Negri IRCCS, Via Mario Negri, 2, 20156, Milano, Italy

^e Humanitas Gavazzeni, Via Gavazzeni, 21, 24125, Bergamo, BG, Italy

ARTICLE INFO

Keywords:

COVID-19 prognostic parameters
Chest computed tomography
Quantitative visual analysis method
Integrated prognostic score
Clinical and laboratory data
Prognostic nomogram

ABSTRACT

Purpose: To evaluate the prognostic role of chest computed tomography (CT), alone or in combination with clinical and laboratory parameters, in COVID-19 patients during the first peak of the pandemic.

Methods: A retrospective single-center study of 301 COVID-19 patients referred to our Emergency Department (ED) from February 25 to March 29, 2020. At presentation, patients underwent chest CT and clinical and laboratory examinations. Outcomes included discharge from the ED after improvement/recovery (positive outcome), or admission to the intensive care unit or death (poor prognosis). A visual quantitative analysis was formed using two scores: the Pulmonary Involvement (PI) score based on the extension of lung involvement, and the Pulmonary Consolidation (PC) score based on lung consolidation. The prognostic value of CT alone or integrated with other parameters was studied by logistic regression and ROC analysis.

Results: The impact of the CT PI score (≥ 15 vs. ≤ 6) on predicting poor prognosis (OR 5.71 95% CI 1.93–16.92, $P = 0.002$) was demonstrated; no significant association was found for the PC score. Chest CT had a prognostic role considering the PI score alone (AUC 0.722) and when evaluated with demographic characteristics, comorbidities, and laboratory data (AUC 0.841). We, therefore, developed a nomogram as an easy tool for immediate clinical application.

Conclusions: Visual analysis of CT gives useful information to physicians for prognostic evaluations, even in conditions of COVID-19 emergency. The predictive value is increased by evaluating CT in combination with clinical and laboratory data.

Abbreviations: CT, computed tomography; COVID-19, Coronavirus Infectious Disease 2019; ED, Emergency Department; ICU, intensive care unit; PI score, Pulmonary Involvement score; PC score, Pulmonary Consolidation score; ROC, Receiver Operating Characteristic; OR, odds ratio; CI, confidence interval; AUC, area under the curve; SARS-CoV-2, severe acute respiratory syndrome coronavirus-2; RSNA, Radiological Society of North America; HIV, Human Immunodeficiency Virus; SaO₂, arterial saturation of oxygen; paO₂, partial pressure of oxygen; pCO₂, partial pressure of carbon dioxide; WBC, white blood cell; ALT, alanine aminotransferase; AST, aspartate aminotransferase; LDH, lactate dehydrogenase; PT, prothrombin time; PTT, partial thromboplastin time; CRP, C-reactive protein level; PCT, procalcitonin; BNP, atrial natriuretic peptide; TnT, troponin levels; SIMIT, Italian Society of Infectious and Tropical Diseases; A.I., Artificial Intelligence.

* Corresponding author.

E-mail addresses: enzo.angeli@gavazzeni.it (E. Angeli), serena.dalto@gavazzeni.it (S. Dalto), stefano.marchese@gavazzeni.it (S. Marchese), lucia.setti@gavazzeni.it (L. Setti), manuela.bonacina@gavazzeni.it (M. Bonacina), francesca.galli@marionegri.it (F. Galli), eliana.rulli@marionegri.it (E. Rulli), valter.torri@marionegri.it (V. Torri), cinzia.monti@gavazzeni.it (C. Monti), roberta.meroni@gavazzeni.it (R. Meroni), giordano.beretta@gavazzeni.it (G.D. Beretta), massimo.castoldi@gavazzeni.it (M. Castoldi), emilio.bombardieri@gavazzeni.it (E. Bombardieri).

<https://doi.org/10.1016/j.ejrad.2021.109612>

Received 12 December 2020; Received in revised form 16 February 2021; Accepted 20 February 2021

Available online 26 February 2021

0720-048X/© 2021 Elsevier B.V. All rights reserved.

1. Introduction

In December 2019, a novel coronavirus, named severe acute respiratory syndrome coronavirus-2 [SARS-CoV-2], emerged in China and has spread globally, creating a pandemic of CoronaVirus Infection Disease (COVID-19). As of the 1st of January 2021, a total of 94,963,847 confirmed cases and a total of 2,050,857 deaths had been reported all over the world [1]. Given the mortality rate of COVID-19 [1–3], the knowledge of potential risk factors associated with a fatal outcome can be considered essential for physicians [4–7]. The present study aimed to contribute to this area.

Chest computed tomography (CT) is a fundamental diagnostic tool for the diagnosis of COVID-19 due to the high sensitivity of CT in depicting interstitial pneumonitis [8]. The role of chest CT is clearly reported by radiological associations such as the Fleischner Society, the American College of Radiology (ACR), the Radiological Society of North America (RSNA), the European Society of Radiology (ESR), the European Society of Thoracic Imaging (ESTI) and the World Health Organization (WHO) [9–15]. Recommendations were made for the use of chest imaging in the care of patients with COVID-19. Chest CT was mainly indicated as an initial diagnostic tool to be used in patients with middle and severe respiratory conditions. Prognostic evaluations and disease monitoring are less frequently reported applications. There is a general agreement that chest imaging combined with clinical evaluation and laboratory tests is essential for correct patient management. Biological parameters provide greatly added value in characterizing the severity of the disease and identifying different orders of risk to predict an unfavorable outcome.

The goal of the present study was to clarify the contribution of CT in the prognostic estimation of COVID-19 pneumonia, using a retrospective evaluation of the very large number of patients referred to our Emergency Department (ED) during the first peak of the pandemic [16]. Our aim was to demonstrate if chest CT was able to predict the outcome of the disease when considered alone or integrated with demographic, clinical and laboratory data. We also wanted to prove the validity of the visual analysis and to generate a prognostic algorithm able to optimize the choice for the most successful individual treatment.

2. Materials and methods

2.1. Patients

Patient selection was carried out among 325 consecutive patients admitted to our ED from February 25 to March 29, 2020, with COVID-19 like symptoms (respiratory symptoms, suspected COVID-19 lung disease, and significant abnormalities on chest X-ray). Patients underwent clinical, radiological and laboratory examinations according to the internal guidelines of our hospital for the management suspected COVID-19. Patients who had a diagnosis of non-COVID-19 lung disease or not undergoing CT at presentation or examined only with chest X-rays were excluded. A total of 301 patients were enrolled. Of these patients, 288 had a confirmed diagnosis of SARS-CoV-2 infection by real-time polymerase chain reaction (RT-PCR) assay from a throat swab specimen. The molecular test was negative in 13 patients. However, the clinical features and the radiological findings allowed physicians to make a diagnosis of COVID-19. In patients who had several CT scans during hospitalization, the first one, at patient admission, was considered for analysis. This study was notified to and approved by our local Ethics Committee as a retrospective. All procedures involving human participants were conducted in accordance with the ethical standards of the institutional and/or national research committee and with the 1964 Helsinki declaration and its later amendments.

2.2. Clinical data collection

At patient presentation, the following parameters were collected:

Table 1

Definition of the Pulmonary Involvement (PI) score and the Pulmonary Consolidation (PC) score.

	PI score (involvement for each lobe)	PC score (consolidation of total lung)
Absent	0	A
≤ 25 %	1	B
26–50%	2	C
51–75%	3	D
76–100 %	4	E

PI score calculator: giving the score to each lobe, the total is the sum of the involvement of the different lobes from 0 to 20.

PC score calculator: considering the total lung, the score is the total of consolidated lung with respect to the total lung.

age, sex, smoking status, diabetes, arterial hypertension, ischemic heart disease, chronic obstructive pulmonary disease, obesity, oncological pathology, autoimmune disease, chronic renal failure, liver disease, human immunodeficiency virus (HIV) and/or bacterial infection. The considered symptoms of COVID-19 were: body temperature, cough, dyspnea, myalgia or malaise or arthralgia, headache, gastrointestinal symptoms, rhinorrhea or conjunctivitis, anosmia or dysgeusia, neurological symptoms. Data on previous domiciliary antibiotic therapy were also reported. Arterial saturation of oxygen (SaO₂) with or without oxygen therapy, heart rate, systolic and diastolic blood pressure were registered.

2.3. Laboratory data collection

The most important tests collected at patient presentation were: partial pressure of oxygen (paO₂) and carbon dioxide (pCO₂), lactate, pH, oxygen therapy, total white blood cell (WBC), neutrophil and lymphocytes counts, hemoglobin, platelets counts, alanine (ALT) and aspartate aminotransferase (AST), bilirubin, lactate dehydrogenase (LDH), creatinine, coagulation time (PT and PTT), fibrinogen, d-dimer, C-reactive protein level (CRP), procalcitonin (PCT), interleukin 6, ferritin, triglyceride, atrial natriuretic peptide (BNP) and troponin levels (TnT). Microbiological data for SARS-CoV-2 were evaluated from nasopharyngeal swabs; blood and urine cultures, pneumococcus and legionella urine tests were also evaluated.

2.4. CT image acquisition and image analysis

Chest CT scans were performed using a multidetector 64-slices CT unit (Siemens Somatom Sensation 64, Siemens Healthineers, Erlangen Germany) and reconstructed at 2.5 mm slice thickness, using both standard lung window (1500 HU width; -500HU center) and soft tissue window (300HU width; 40HU center). All patients were scanned in the supine position, during inspiratory breath-hold, from the apex to the lung bases. CT examinations were performed without contrast administration, except in some patients with suspected pulmonary embolism after the initial clinical and laboratory assessment (D-dimer). In these cases, the CT study was integrated with a regular injection protocol for pulmonary artery evaluation. CT images were retrospectively and independently evaluated by two radiologists with more than 5 years of experience of chest imaging, blinded to clinical data and laboratory tests. In the case of disagreement, a consensus was obtained by consulting a third radiologist with 20 years of experience. In each CT study, the severity of pneumonia was graded using two previously created prognostic scores (PI score and PC score) as described below. In order to provide better quantification of lung abnormalities, regular multiplanar reconstruction images in coronal and sagittal planes were used. No specific automated or semi-automated software for lung segmentation was applied.

2.5. Radiological score (PI and PC score)

For each chest CT, each lung lobe (right upper lobe, right middle lobe, right lower lobe, left upper lobe, and left lower lobe) was assessed. As summarized in Table 1, lung involvement was studied by two different scores: a) a quantitative score, the Pulmonary Involvement (PI) score, based on the extension of lung involvement; and b) a qualitative score, the Pulmonary Consolidation (PC) score, describing the rate on lung consolidation. The PI score was calculated by assigning to each lobe a number from 0 to 4, expressing the extent of the parenchymal involvement, regardless of the findings of ground-glass opacities, crazy paving or parenchymal consolidation as described by the international standard nomenclature according to the Fleischner Society Glossary [9]. The rate of involvement for each lung lobe was scored on a five-degree scale: 0: no involvement; 1: $\leq 25\%$; 2: 26–50%; 3: 51–75%; 4: 76–100% of involvement. The sum of all lobe scores allowed us to obtain the final PI score ranging from 0 to 20. Parenchymal involvement was subgrouped as follows: no involvement, mild involvement (PI score from 1 to 6); moderate involvement (PI score from 7 to 10); severe involvement (PI score from 11 to 14); massive involvement (PI score from 15 to 20). The PC score was calculated by evaluating the consolidated portion of the affected lung and expressing with letters A, B, C, D, E the percentage of the consolidated lung compared to the overall affected parenchyma, as follows: A: no consolidation; B: $\leq 25\%$ consolidation; C: 26–50% consolidation; D: 51–75% consolidation; E: 76–100% consolidation.

2.6. Treatment

Patients admitted to the ED and ICU were treated according to the guidelines of the Italian Society of Infectious and Tropical Diseases (SIMIT). During the first phase of pandemic the recommended therapy was hydroxychloroquine, various antiviral agents, steroids, low molecular weight heparin and ventilator support in different combinations according to the clinician's evaluation. The antibiotic therapy was adopted only in case of suspected or confirmed superinfection. The application of these protocols, published on the website of the Society (see: <https://www.simit.org/images/news/1588-flow-chart-gestionale-terapia-domiciliare-precocoe-covid-19-versione-27-marzo-2020.pdf>), has changed over time, as, in the early phases of the pandemic when little was known about the viral infection, there were no standard treatments. However, the treatment given was considered in this analysis because it is an important factor influencing the prognosis.

2.7. Definition of endpoint

To classify the group of patients examined, we considered a poor prognosis to be admission to the intensive care unit (ICU) or death. A positive outcome was defined as those patients who had either discharge or were transferred to regular ward care.

2.8. Statistical analysis

Continuous variables concerning the laboratory test results were categorized according to the normal range values; in case all or almost all observed values were out of range, the median or tertiles of the observed distribution were used. No imputation of missing data was planned.

The role of radiological results was investigated by means of univariable and multivariable logistic regression models. Statistically significant variables at the univariable logistic analysis were considered for the multivariable model only in case of not having more than 10% of missing data. The stepwise procedure was implemented to select the variables to include in the final multivariable model, taking the radiological variables fixed in the model. The patients with missing data for one or more variables included in the final multivariable model were

Table 2
Patient characteristics.

	Improvement/ Recovery (N = 177)	Worsening/ ICU/ Death (N = 124)	Overall (N = 301)
Demographic and clinical characteristics			
Age			
Mean (SD)	66.3 (13.4)	74.8 (10.5)	69.8 (13.0)
Median (Q1 - Q3)	65.7 (57.4–77.8)	76.2 (69.3–82.4)	71.4 (61.0–79.6)
Min - Max	29.4 - 98.0	47.0 - 96.7	29.4 - 98.0
Sex			
Male	113 (63.8)	96 (77.4)	209 (69.4)
Female	64 (36.2)	28 (22.6)	92 (30.6)
Arterial hypertension			
Missing	0	1	1
No	94 (53.1)	46 (37.4)	140 (46.7)
Yes	83 (46.9)	77 (62.6)	160 (53.3)
Ischemic heart disease			
Missing	0	1	1
No	155 (87.6)	97 (78.9)	252 (84.0)
Yes	22 (12.4)	26 (21.1)	48 (16.0)
Symptoms			
Body temperature (°C)			
Median (Q1 - Q3)	37.7 (37.0–38.2)	37.8 (37.0–38.5)	37.7 (37.0–38.3)
Min - Max	36.0 - 40.1	36.0 - 40.1	36.0 - 40.1
Missing	0	1	1
Cough			
No	88 (49.7)	57 (46.0)	145 (48.2)
Yes	89 (50.3)	67 (54.0)	156 (51.8)
Dyspnea			
No	55 (31.1)	26 (21.0)	81 (26.9)
Yes	122 (68.9)	98 (79.0)	220 (73.1)
Myalgia/malaise/arthralgia			
No	122 (68.9)	92 (74.2)	214 (71.1)
Yes	55 (31.1)	32 (25.8)	87 (28.9)
Headache			
No	172 (97.2)	123 (99.2)	295 (98.0)
Yes	5 (2.8)	1 (0.8)	6 (2.0)
Gastrointestinal symptoms			
No	151 (85.3)	100 (80.6)	251 (83.4)
Yes	26 (14.7)	24 (19.4)	50 (16.6)
Neurological symptoms			
No	147 (83.1)	103 (83.1)	250 (83.1)
Yes	30 (16.9)	21 (16.9)	51 (16.9)
Laboratory exams			
SaO2 (%)			
Median (Q1 - Q3)	90.0 (86.0–94.0)	85.0 (76.0–91.0)	88.0 (83.0–93.0)
Min - Max	58.0 - 99.0	52.0 - 100.0	52.0 - 100.0
Missing	8	14	22
paO2 (mmHg)			
Median (Q1 - Q3)	58.0 (50.0–69.0)	51.0 (41.0–64.0)	55.0 (46.5–66.0)
Min - Max	35.0 - 336.0	22.0 - 99.0	22.0 - 336.0
Missing	38	15	53
Lactate (mmol/L)			
Median (Q1 - Q3)	1.0 (0.8–1.5)	1.4 (1.0–2.1)	1.2 (0.9–1.7)
Min - Max	0.4 - 15.0	0.5 - 8.3	0.4 - 15.0
Missing	40	16	56
WBC ($\times 10^3/\text{mml}$)			
Median (Q1 - Q3)	6.25 (4.8–8.7)	7.3 (5.4–10)	6.5 (5–9)
Min - Max	2.4 - 2.95	1.7 - 3.57	1.7 - 3.57
Missing	1	0	1
Neutrophil count ($\times 10^3/\text{mml}$)			
Median (Q1 - Q3)	4.5 (3.6–7.1)	5.8 (4.1–8.35)	5.3 (3.75–7.6)
Min - Max	0.7 - 24.2	0.9 - 16.2	0.7 - 24.2
Missing	1	0	1

(continued on next page)

Table 2 (continued)

	Improvement/ Recovery (N = 177)	Worsening/ ICU/ Death (N = 124)	Overall (N = 301)
Lymphocytes count (x 10³/mmc)			
Median (Q1 - Q3)	0.9 (0.6–1.15)	0.7 (0.5–1)	0.8 (0.6–1.1)
Min - Max	0.1 - 4	0.2 - 29	0.1 - 29
Missing	1	0	1
AST (U/L)			
Median (Q1 - Q3)	39.5 (28.0–58.0)	50.0 (36.0–77.0)	44.0 (31.0–65.0)
Min - Max	12.0 - 593.0	14.0 - 233.0	12.0 - 593.0
Missing	1	1	2
ALT (U/L)			
Median (Q1 - Q3)	28.5 (20.0–45.0)	30.5 (19.0–50.0)	29.0 (20.0–48.0)
Min - Max	4.0 - 608.0	2.0 - 196.0	2.0 - 608.0
Missing	1	0	1
LDH (U/L)			
Median (Q1 - Q3)	319.5 (237.0–415.0)	444.5 (325.0–613.0)	364.5 (258.0–491.0)
Min - Max	136.0 - 1321.0	168.0 - 5400.0	136.0 - 5400.0
Missing	33	30	63
D-dimer (ng/mL)			
Median (Q1 - Q3)	1404.0 (978.0–2364.0)	1959.0 (1073.0–5064.0)	1603.0 (978.0–2845.0)
Min - Max	179.0 - 23086.0	576.0 - 35054.0	179.0 - 35054.0
Missing	87	83	170
CRP (mg/dL)			
Median (Q1 - Q3)	10.1 (4.9–15.3)	14.4 (8.0–20.3)	11.4 (5.8–17.8)
Min - Max	0.1 - 42.5	0.6 - 41.0	0.1 - 42.5
Missing	1	3	4
PCT (ng/mL)			
Median (Q1 - Q3)	0.1 (0.1–0.4)	0.4 (0.2–1.1)	0.2 (0.1–0.6)
Min - Max	0.0 - 64.3	0.1 - 81.2	0.0 - 81.2
Missing	41	36	77
Microbiology investigations			
First nasopharyngeal swab for COVID-19			
Negative	24 (13.6)	15 (12.1)	39 (13.0)
Positive	152 (86.4)	109 (87.9)	261 (87.0)
Missing	1	0	1
Second nasopharyngeal swab for COVID-19			
Negative	10 (5.7)	2 (1.6)	12 (4.0)
Positive	13 (7.4)	9 (7.3)	22 (7.3)
Not performed	153 (86.9)	113 (91.1)	266 (88.7)
Missing	1	0	1

Abbreviations: SD, standard deviation; Q1-Q3, first-third quartile; SaO₂, arterial saturation of oxygen; paO₂, partial pressure of oxygen; ICU, intensive care unit; WBC, white blood cell; AST, aspartate aminotransferase; ALT, alanine aminotransferase; LDH, lactate dehydrogenase; CRP, C-reactive protein level; PCT, procalcitonin; COVID-19, Coronavirus Infectious Disease 2019.

excluded from the multivariable analysis. Results were expressed in terms of odds ratios (ORs) and their 95 % confidence interval (95 % CI).

The model accuracy was evaluated by means of a ROC (Receiver Operating Characteristic) curve and calculating the area under the curve (AUC) with its 95 % CI. Comparisons between the accuracy of the models in terms of AUC were performed by means of a chi-squared test.

A nomogram was developed to display the predicted probability of worsening of the disease. To define the multivariable model, the same method described above was used, but the treatment administered was not considered for the selection of variables, and the radiological scores were not forced to be included in the model. Since the exclusion of the treatment administered as an independent variable could decrease the model accuracy, the difference in terms of AUC between the models including or excluding this variable was calculated and analyzed as described above.

A *P*-value <0.05 was considered to be statistically significant. Analyses were carried out using SAS statistical software (version 9.4).

Table 3

Radiological results, therapy and outcome.

	Improvement/ Recovery (N = 177)	Worsening/ ICU/ Death (N = 124)	Overall (N = 301)
Radiological PI score			
Missing			1
Up to 6	58 (33.0)	21 (16.9)	79 (26.3)
7–10	61 (34.7)	23 (18.5)	84 (28.0)
11–14	43 (24.4)	33 (26.6)	76 (25.3)
≥15	14 (8.0)	47 (37.9)	61 (20.3)
Radiological PC score			
Missing			2
A	87 (49.7)	37 (29.8)	124 (41.5)
B	51 (29.1)	62 (50.0)	113 (37.8)
C, D, E	37 (21.1)	25 (20.2)	62 (20.7)
Oxygen therapy			
Missing	39	15	54
No	108 (78.3)	65 (59.6)	173 (70.0)
Yes	30 (21.7)	44 (40.4)	74 (30.0)
Oxygen (L)			
Mean (SD)	8.5 (4.8)	10.2 (4.6)	9.5 (4.7)
Median (Q1 - Q3)	7.0 (6.0–15.0)	12.0 (6.0–15.0)	8.0 (6.0–15.0)
Min - Max	2.0 - 15.0	2.0 - 15.0	2.0 - 15.0
Missing	8	12	20
SIMIT therapy			
No	63 (35.6)	63 (50.8)	126 (41.9)
Yes	114 (64.4)	61 (49.2)	175 (58.1)
Outcome			
Improvement/ recovery	177 (100.0)	0 (0.0)	177 (58.8)
Worsening/ intensive care unit	0 (0.0)	32 (25.8)	32 (10.6)
Death	0 (0.0)	92 (74.2)	92 (30.6)

Abbreviations: SD, standard deviation; Q1-Q3, first-third quartile; ICU, intensive care unit; PI score, pulmonary involvement score; PC score, pulmonary consolidation score; L, liters per minute; SIMIT, Italian Infectious Disease Society.

3. Results

Between February 25 to March 29, 2020, during the first peak of the pandemic, 325 patients were admitted to the ED of our hospital for COVID-19-like symptoms. Of these, 24 patients were excluded from our retrospective analysis because chest CT was not performed at patient presentation or the diagnosis of COVID-19 was not confirmed. Therefore, 301 patients were included in the present analysis. Regarding the CT protocol, 38 out of 301 patients (12.6 %) had contrast-enhanced studies to rule out pulmonary embolism.

Table 2 reports the main demographic and clinical characteristics of included patients and the main laboratory tests performed. Full details are provided in Supplementary Table S1.

Overall, 221 (73.6 %) patients had a PI score higher than 6, and 61 (20.3 %) had a PI score of 15 or higher, while a PC score equal to A was observed in 124 (41.5 %) patients (Table 3). Examples of CT scans in these patients are shown in Fig. 1. Oxygen therapy was administered to 74 (30.0 %) patients, 175 (58.1 %) were treated according to the SIMIT protocol, while 126 (41.9 %) received only best supportive care. Improvement or complete recovery of disease was observed for 177 (58.8 %) patients, while 32 (10.6 %) patients experienced a deterioration of clinical condition or ICU admission and 92 (30.6 %) died. Therefore, a worsening of disease occurred in 124 (41.2 %) patients.

At univariable analysis, a statistically significant association with risk of disease worsening was identified for both PI score [11–14 vs. 6] (OR 2.12, 95 % CI 1.08–4.16, *P* = 0.029); PI score [≥15 vs. ≤ 6] (OR 9.27, 95 % CI 4.26–20.2, *P* < 0.001).

All univariable analysis results are provided in Supplementary Table S2, while significant associations are shown in Table 4.

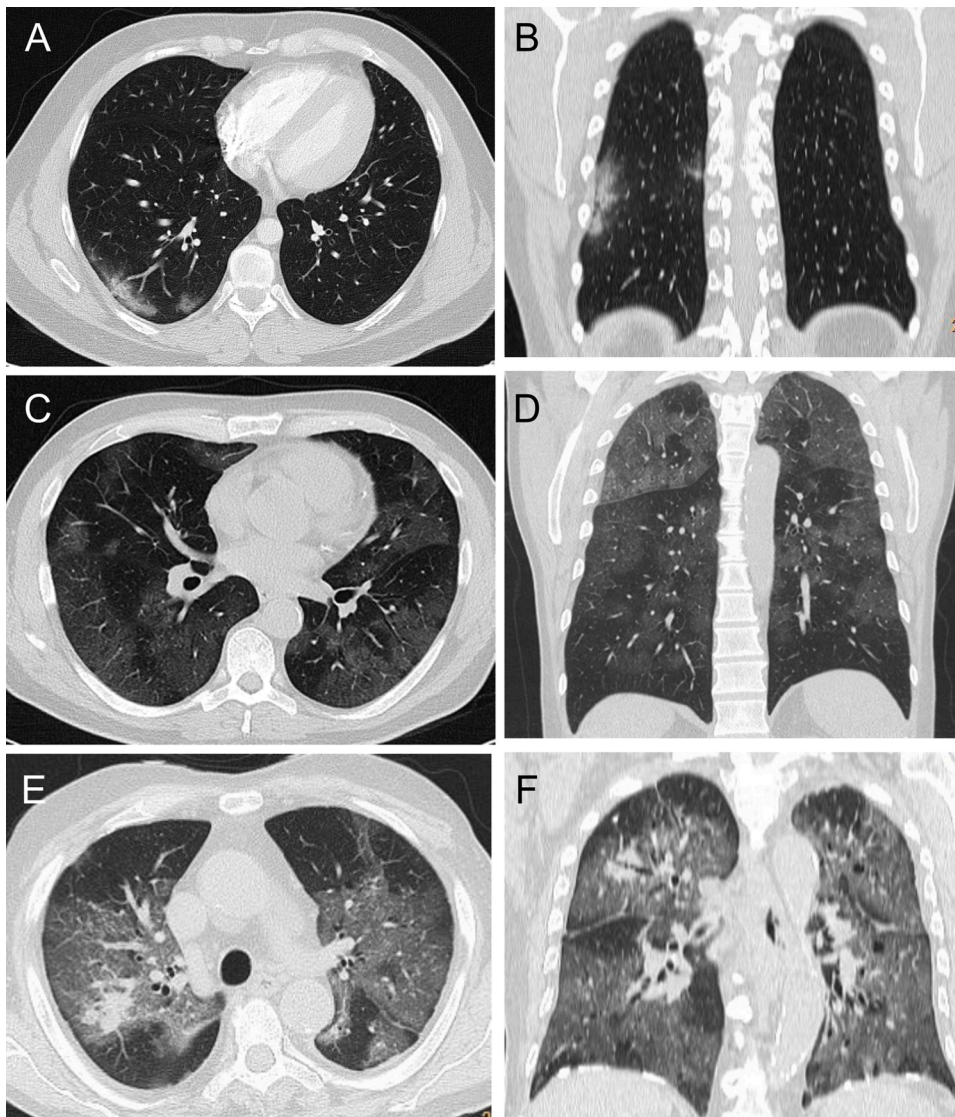


Fig. 1. Examples of CT images from patients with Covid-19 pneumonia. Axial image and coronal reconstruction in A), B): a patient showing minimal involvement, peripheral ground-glass opacities exclusively in the right lower lobe, PI score 1, PC score A. C), D): a patient with severe involvement, showing bilateral wide areas of ground-glass opacities, PI score 14, PC score A. E), F): a patient with massive lung involvement, showing near total extension of the pneumonia, and only mild consolidation in the right upper lobe, PI score 18, PC score B.

Abbreviations: CT, computed tomography; PC score, lung consolidation score; PI score, lung involvement score.

Although significant at univariable analysis, the following variables were not considered due to a missing data proportion higher than 10 %: SaO₂ with oxygen therapy, paO₂, lactate, LDH, PT, PTT, PCT, BNP, TnT, oxygen therapy. Ischemic heart disease, oncological pathology, lymphocytes count and CRP were not selected by the stepwise procedure. Among 301 patients, 25 were excluded from the multivariable analysis due to missing data for some variables (i.e., radiological scores, arterial hypertension, SaO₂ and the WBC and AST values). No significant differences in the collected characteristics were detected between the subgroup of 276 patients included in the multivariable analysis and the whole sample (data not shown).

Results of the multivariable analyses are reported in Table 5. The impact of the PI score on the risk of disease worsening was confirmed (OR $_{\geq 15 \text{ vs. } \leq 6}$ 5.71, 95 % CI 1.93–16.92, $P = 0.002$), whereas no statistically significant association was found for PC score. A statistically significant higher risk of a worse prognosis was found for older and male patients. A SaO₂ lower than 85 %, and high levels of WBC and AST were confirmed as statistically significant risk factors. A statistically significant positive impact on prognosis was found for patients treated according to the SIMIT therapy protocol. The contribution of radiological scores was analyzed comparing the AUC of the final model (0.844, 95 % CI 0.797–0.891) with the AUC of the model including only PI and PC (AUC = 0.744) and the model with all variables except PC score

(AUC = 0.841) (Fig. 2). The AUC difference was -0.100 ($P < 0.001$) and -0.003 ($P = 0.498$) for the first and the second model, respectively.

Results of the multivariable model implemented to define the prognostic score to predict the disease worsening are reported in Table 5. It includes all the variables selected in the multivariable model described above except the radiological PC score and the SIMIT therapy. The AUC calculated for this model was 0.839 (95 % CI 0.792–0.886), whereas the AUC of the model that also included the SIMIT therapy was 0.842 (95 % CI 0.800–0.889). No statistically significant difference was detected ($P = 0.670$).

The nomogram (Fig. 3) shows the probability of the worsening of disease according to age, sex, SaO₂, arterial hypertension, PI score, WBC count and AST levels. For each factor, based on the risk category, a score is assigned and the sum of the seven scores plotted on the “total points” line corresponds to the probability of disease worsening, plotted on the “risk of event” axis.

4. Discussion

The role of CT for the diagnosis of COVID 19 interstitial pneumonia is well established. The typical imaging patterns of lung abnormalities in patients with lung involvement have been described. The presence of multiple bilateral patchy ground-glass opacities with multilobular and

Table 4

Impact on the risk of disease worsening of radiological results and demographical-clinical characteristics, laboratory tests and therapy. Univariable logistic regression models.

	N	OR (95 % CI)	P-value
Radiological PI score (ref. Up to 6)	300		<0.001*
7–10		1.04 (0.52–2.08)	0.909
11–14		2.12 (1.08–4.16)	0.029*
≥15		9.27 (4.26–20.2)	<0.001*
Radiological PC score (ref. A)	299		<0.001*
B		2.86 (1.68–4.88)	<0.001*
C, D, E		1.59 (0.84–3.00)	0.154
Age (ref. < 65 years)	301		<0.001*
65–80		2.97 (1.67–5.31)	<0.001*
> 80 years		5.22 (2.68–10.2)	<0.001*
Male sex (ref. Female)	301	1.94 (1.15–3.27)	0.013*
Arterial hypertension	300	1.90 (1.19–3.03)	0.008*
Ischemic heart disease	300	1.89 (1.01–3.52)	0.045*
Oncological pathology (ref. No/Previous)	296	2.05 (1.02–4.12)	0.043*
SaO₂ (ref. 95 %–100 %)	279		<0.001*
85 %–94 %		1.86 (0.86–4.04)	0.116
<85 %		7.57 (3.30–17.4)	<0.001*
SaO₂ < 95 % with oxygen therapy (ref. 95 %–100 %)	235	1.69 (1.01–2.84)	0.046*
paO₂ (ref. ≥ 80 mmHg)	248		0.016*
<54 mmHg		2.99 (1.00–8.94)	0.050*
54–79 mmHg		1.53 (0.51–4.59)	0.447
Lactate >2.2 mmol/L (ref. ≤ 2.2 mmol/L)	245	2.66 (1.25–5.67)	0.011*
Oxygen therapy (ref. Aria ambient)	227		0.007*
Oxygen, L less than median		1.36 (0.53–3.46)	0.519
Oxygen, L more than median		3.47 (1.59–7.59)	0.002*
WBC >10000/mm³ (ref. ≤ 10000/mm ³)	300	2.10 (1.17–3.77)	0.013*
Lymphocytes (ref. > 1000/mm ³)	300		0.016*
<700/mm ³		2.34 (1.28–4.26)	0.006*
700–1000/mm ³		1.34 (0.74–2.40)	0.332
AST ≥50 U/L (ref. < 50 U/L)	299	2.19 (1.36–3.52)	0.001*
LDH (ref. <248 U/L)	238		<0.001*
248–400 U/L		2.45 (1.06–5.66)	0.036*
>400 U/L		6.03 (2.64–13.8)	<0.001*
PT > 1.18 (ref. ≤ 1.18)	261	1.92 (1.06–3.48)	0.032*
PTT > 1.2 (ref. ≤ 1.2)	260	3.28 (1.90–5.65)	<0.001*
CRP (ref. 7.6–15.3 mg/dL)	297		<0.001*
<7.6 mg/dL		0.64 (0.35–1.16)	0.142
>15.3 mg/dL		2.22 (1.26–3.92)	0.006*
PCT (ref. 0.11–0.38 ng/mL)	224		<0.001*
<0.11 ng/mL		0.35 (0.17–0.75)	0.007*
>0.38 ng/mL		2.20 (1.15–4.19)	0.017*

Table 4 (continued)

	N	OR (95 % CI)	P-value
BNP (ref. 42–127 pg/mL)	105		0.048*
<42 pg/mL		0.22 (0.06–0.88)	0.032*
>127 pg/mL		1.19 (0.44–3.21)	0.737
Tnt (ref. <11.6 ng/L (female), <19.8 ng/L (male))	160		<0.001*
≥11.6 ng/L (female), ≥19.8 ng/L (male)		4.40 (2.22–8.74)	<0.001*
SIMIT therapy	301	0.54 (0.34–0.85)	0.009*

Abbreviations: OR, odds ratio; 95 % CI, 95 % confidence interval; PI score, pulmonary involvement score; PC score, pulmonary consolidation score; SaO₂, arterial saturation of oxygen; paO₂, partial pressure of oxygen; WBC, white blood cell; AST, aspartate aminotransferase; LDH, lactate dehydrogenase; PT, prothrombin time PTT, thromboplastin time CRP, C-reactive protein level; PCT, procalcitonin; BNP, atrial natriuretic peptide; TnT, troponin levels; SIMIT, Italian Infectious Disease Society.

peripheral distribution is common; less frequently, images of consolidation, reticular pattern, and vascular signs can be seen [4,8,16–18]. The Fleischner Society issued a consensus statement in order to explore the best application of imaging, primarily CT, for the evaluation and risk stratification of patients [10], acknowledging that, in addition to supporting diagnosis, CT has also revealed its usefulness for providing diagnostic information. This approach requires the quantification of abnormalities that currently can be reached through visual analysis [19–23], or more recently using a software-based assessment [24–27] or, possibly in the future, artificial intelligence (A.I.) [28–30].

The present study was retrospectively carried out on a series of 301 chest CT scans performed at presentation in the ED, and, focusing on the prediction of the outcome of patients in such severe conditions of emergency, we also analyzed the weight of clinical and laboratory parameters. This choice allowed us to investigate both the prognostic value of a CT scan alone and in association with clinical and laboratory tests. Two different lung scores (PI and PC scores) were constructed to measure extension (PI) and consolidation (PC) of parenchymal involvement. PI and PC scores in the univariable analysis showed significant prognostic value, but only the PI score confirmed its role in multivariable analysis. In other words, the most useful prognostic CT sign in predicting the outcome of COVID-19 patients was the expression of global lung involvement, regardless of the type of alteration and the consolidation density of the images. Although some recent papers [25–27] described some results on quantification based on open-source software for semi-automated pulmonary segmentation, in our experience, the visual analysis of lung involvement proved to be a quick, easy-to-use and reliable method for the evaluation and quantitation of lung involvement. This procedure can also be used also in an emergency scenario, independently of sophisticated, different, and still not fully comparable software-based methods for the interpretation of CT images. Despite a recent rapid increase of studies using A.I. for the diagnosis of COVID-19 lung opacities, at present, the application in the area of prediction of unfavorable outcome is still very preliminary [30].

Few retrospective studies have evaluated the correlation between thorax imaging and clinical outcome in patients with COVID-19 pneumonia; a radiographic severity index based on Chest X-ray has been proposed by some authors [34,37]. The importance of thorax CT features in the early phase of COVID-19 in determining the severity of the disease was reported in some papers [31–33,35–37]. The necessity of considering clinical and laboratory parameters together with radiological findings was shown to be evident, because their evaluation at patient presentation can contribute to better defining the severity of COVID-19 infection. Therefore, we decided to investigate the added value of this combination.

The mean age of our sample was 69.8 years, and the majority of

Table 5
Impact on the risk of disease worsening. Multivariable logistic regression model including (model 1) or excluding SIMIT therapy (model 2).

	Multivariable model 1 ^a (276 patients, 109 events)		Multivariable model 2 ^b (277 patients, 109 events)		Points ^c
	OR (95 % CI)	P-value	OR (95 % CI)	P-value	
Radiological PI score (ref. Up to 6)		0.006*		0.004*	
7–10	1.12 (0.46–2.75)	0.798	1.10 (0.46–2.63)	0.836	4
11–14	1.71 (0.67–4.39)	0.262	1.76 (0.72–4.27)	0.213	26
≥15	5.71 (1.93–16.92)	0.002*	5.86 (2.06–16.65)	0.001*	80
Radiological PC score (ref. A)		0.485			
B	1.50 (0.70–3.21)	0.292	Not included		
C, D, E	1.56 (0.66–3.67)	0.308			
Age (ref. < 65 years)		0.001*		<0.001*	
65–80	3.09 (1.43–6.67)	0.004*	3.04 (1.44–6.42)	0.004*	50
>80 years	5.71 (2.12–15.35)	0.001*	9.07 (3.65–22.55)	<0.001*	100
Male sex (ref. Female)	2.72 (1.34–5.50)	0.006*	2.66 (1.34–5.31)	0.005*	44
Arterial hypertension	1.54 (0.81–2.95)	0.189	1.58 (0.83–2.98)	0.163	21
SaO2 (ref. 95 %–100 %)		0.025*		0.024*	
85 %–94 %	1.79 (0.70–4.57)	0.221	1.60 (0.64–4.03)	0.315	21
<85 %	4.32 (1.42–13.15)	0.010*	3.95 (1.34–11.66)	0.013*	62
WBC >10000/mmc (ref. ≤ 10000/mmc)	2.26 (1.04–4.89)	0.039*	2.07 (0.98–4.36)	0.055	33
AST ≥50 U/L (ref. < 50 U/L)	2.15 (1.10–4.21)	0.025*	2.10 (1.10–4.01)	0.025*	34
SIMIT therapy	0.41 (0.19–0.89)	0.024*	Not included		

Abbreviations: SIMIT, Italian Infectious Disease Society; OR, odds ratio; 95 % CI, 95 % confidence interval; PI score, pulmonary involvement score; PC score, pulmonary consolidation score; SaO2, arterial saturation of oxygen; WBC, white blood cell; AST, aspartate aminotransferase.

^a Variables not selected with stepwise procedure: Ischemic heart disease, oncological pathology, lymphocytes, CRP.

^b Variables not selected with a stepwise procedure: ischemic heart disease, oncological pathology, lymphocytes, CRP, radiological score PC.

^c Points associated with the reference category were 0.

* Statistically significant.

patients (69.4 %, 209 patients) were male. The univariable and multivariable analysis confirmed that both of these demographic features had a significant prognostic role ($P < 0.001$ for age, 0.005 for sex) as described in the literature [31,32]. None of the symptoms showed a prognostic impact, although dyspnea was the most frequent symptom observed (73.1 %) in our study, and showed some impact at univariable analysis (OR 1.70, 95 % CI 0.99–2.91, $P = 0.053$), as suggested by the literature [38–40]. In these analyses, cough and body temperature > 37.5 °C were less frequent than what has been described in the literature for Chinese patients [41–43]. This may be because some patients were frightened by the Chinese experience and therefore went to ED at the first symptoms, without waiting for worsening of respiratory distress or hyperpyrexia.

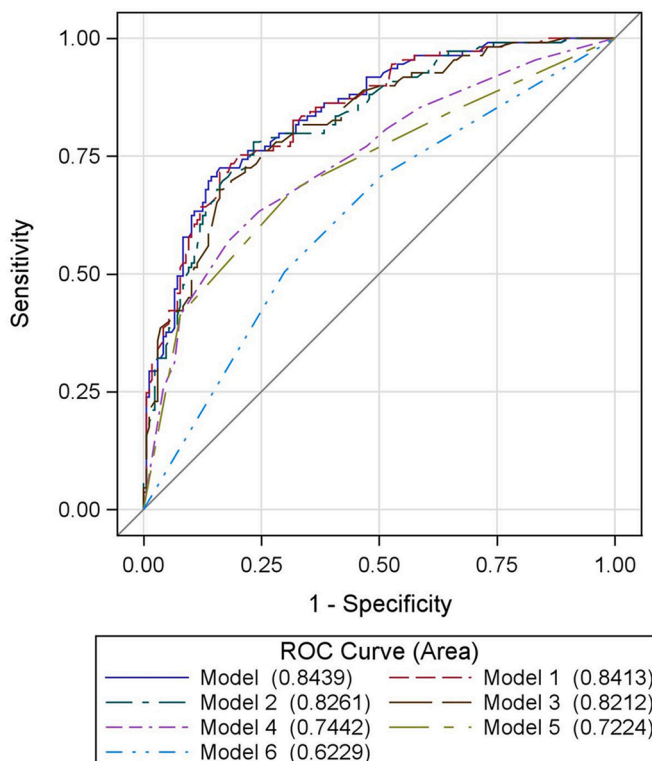
Looking at comorbidities, at univariable analysis only arterial hypertension (OR 1.90, 95 % CI 1.19–3.03, $P = 0.008$), ischemic heart disease (1.89, 95 % CI 1.89, 95 % CI 1.01–3.52, $P = 0.045$) and oncological disease (OR 2.05, 95 % CI 1.02–4.12, $P = 0.043$) showed prognostic significance in our series, not confirmed by multivariable analysis. Similar results have been reported by others [38–40]. However, in these studies, diabetes had no impact and smoking exposure did not emerge as an independent risk factor. In this regard [37,44–46], we noticed only a limited number of smokers in our group of patients (4.6 %, 9 patients). Regarding the laboratory data, many variables demonstrated a statistically significant association with the prognosis, as in Chinese studies [39–42] and an American review [31], but we found a significant prognostic value only for SaO2, WBC, and AST.

As a result of this multiparametric approach, the possible role of radiology in early disease in predicting an adverse outcome was confirmed. The quantitative visual analysis of chest CT scans showed a prognostic role when considering PI score alone (AUC 0.722). Its accuracy increased (AUC 0.841) when evaluated together with some demographic characteristics (age and sex), comorbidities (hypertension) and laboratory data (WBC and AST).

The data collected allowed us to generate a nomogram in order to have an easy clinical practice tool able to guide the choice of physicians in particular critical cases between intensive treatment or best supportive care.

To our knowledge, only two recent retrospective studies have

proposed the construction of a nomogram in order to identify the predictors of severe coronavirus disease [47,48]. The first study used multivariate analysis to evaluate various clinical and laboratory parameters. Age, fever, overweight, polypnea, CPR, troponin, and lymphopenia were retained as risk factors of an unfavorable outcome, and a nomogram was established with sufficient discriminatory power. However, the author did not include CT imaging among the risk indicators [47]. In contrast, CT was considered in the second paper, where initial clinical data and CT imaging data were evaluated in 217 COVID-19 patients [48]. Patients were classified into two groups; mild and severe disease. Multivariate statistic regression determined the independent risk factors associated with severe disease, and selected variables for the nomogram to predict an unfavorable outcome. This nomogram, incorporating both clinical and CT characteristics, was validated on a cohort of the same population, and demonstrated high accuracy in predicting the worst prognosis. However, this approach has to be considered in the light of the selected sample, in which 212 of 219 patients were discharged and only five patients died. Thus the disease severity does not represent what was described in an ED during a peak of the pandemic, whereas our nomogram was based on data obtained from a population of patients admitted to our Hospital in very critical conditions [15]. A limitation of our study is its monocentric and retrospective nature, and, consequently, the results should be related to the characteristics of our series of patients and their management. Moreover, although the patients were included consecutively, we were not able to provide a complete flowchart of the patients' selection. For this reason, a selection bias cannot be completely excluded. Some patients at presentation were not studied using CT, and several laboratory data were missing in some patients. This might be due both to the emergency situation and the severe clinical conditions of some patients. An additional potential limitation is a lack of data on the variability and reproducibility of the CT readers in imaging scoring. However, this was partly overcome by the fact that images were retrospectively and independently evaluated by two radiologists, and any eventual disagreement was resolved by consultation with a third experienced senior radiologist. Finally, the individual therapy administered to patients was not detailed because in such conditions, our physicians followed the SIMIT protocols. In that period, the SIMIT guidelines included many options, and



Model	AUC	95% CI	Difference	95% CI	p-value
Final model: All variables	0.844	0.797-0.891		Reference	
Model 1: All variables except score PC	0.841	0.795-0.888	-0.0026	-0.0100 to 0.0048	0.498
Model 2: All variables except score PI	0.826	0.777-0.876	-0.018	-0.039 to 0.0038	0.106
Model 3: All variables except score PI and score PC	0.821	0.771-0.871	-0.023	-0.047 to 0.0011	0.061
Model 4: Only score PI and score PC	0.744	0.684-0.804	-0.100	-0.150 to -0.049	<0.001
Model 5: Only score PI	0.722	0.661-0.784	-0.122	-0.176 to -0.067	<0.001
Model 6: Only score PC	0.623	0.560-0.686	-0.221	-0.287 to -0.1548	<0.001

Fig. 2. Model accuracy comparison (276 patients, 109 events). Abbreviations: AUC, area under the curve; 95 % CI, 95 % confidence interval; PC score, lung consolidation score; PI score, lung involvement score.

changed over the course of the study. In the period of the peak of the COVID-19 pandemic, any proposed treatment considered appropriate was approved for use by the internal COVID-19 Emergency Committee. Besides this, it should be underlined that some specific strategies of treatment were often adopted for individual patients, after evaluation of the severity of their conditions and calculating the best chances of response in that critical situation.

In conclusion, our study carried out on COVID-patients during the first dramatic phase of the COVID-19 outbreak confirms the potential role of visual quantitative analysis of chest CT performed at disease presentation in predicting the patient outcome. The comprehensive evaluation of radiological data integrated with clinical and laboratory parameters was shown to significantly enhance the combined predictive power and allowed the construction of an original nomogram.

Funding

This paper was partially supported by the Fondazione Humanitas per la Ricerca and by the private donation from Antonella Manera in memory of her parents Mariuccia and Giovanni.

Ethical approval

All procedures followed were in accordance with the ethical standards of the responsible committee on human experimental and with the Helsinki Declaration of 1975, revised in 2008.

Methodology

Retrospective, observational, unicenter study.

Guarantor

The scientific guarantor of this publication is Emilio Bombardieri.

Statistics and biometry

The statistical analysis was performed by Laboratory of Methodology for Clinical Research, Istituto di Ricerche Farmacologiche Mario Negri IRCCS, Milano, Italy.

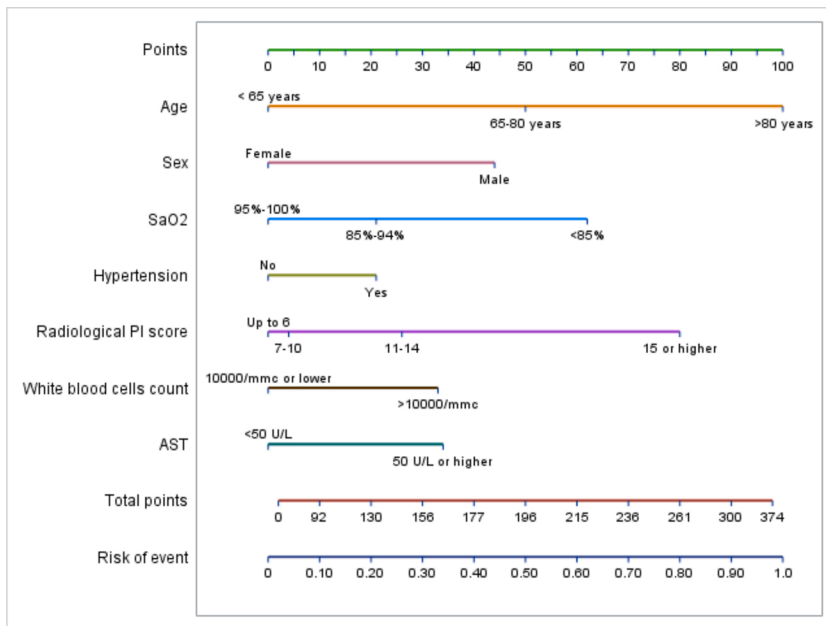


Fig. 3. Nomogram for risk of disease worsening. The nomogram shows the probability of the worsening of disease according to age, sex, SaO₂, arterial hypertension, PI score, WBC count and AST levels. For each factor, based on the risk category, a score is assigned (“points” line). The sum of the seven scores plotted on the “total points” line corresponds to the probability of disease worsening, plotted on the “risk of event” axis. For example, for a patient with all risk factors, the points are: 100 for age > 80 years, 44 for male sex, 21 for arterial hypertension, 80 for a PI score > 15, 62 for a SaO₂ < 85 %, 33 for a WBC count > 10000/mmc, 34 for AST levels > 50 U/L. The total score is 374, corresponding to a disease worsening probability of 98 %. In contrast, a patient with arterial hypertension but no other risk factor reaches a total score of 21 and a disease worsening probability of about 2%.

Abbreviations: AST, aspartate aminotransferase; PC score, lung consolidation score; PI score, lung involvement score; SaO₂, arterial saturation of oxygen; ROC, Receiver Operating Characteristic; WBC, white blood cells.

Informed consent

This study was notified to our local ethics committee as a retrospective analysis. According to the retrospective nature of this study, the need to obtain informed consent was waived by the Institutional Review Board.

CRediT authorship contribution statement

Enzo Angeli: Conceptualization, Methodology, Investigation, Supervision. **Serena Dalto:** Methodology, Formal analysis, Investigation, Data curation. **Stefano Marchese:** Investigation, Visualization. **Lucia Setti:** Investigation, Data curation. **Manuela Bonacina:** Investigation, Data curation. **Francesca Galli:** Formal analysis. **Eliana Rulli:** Formal analysis. **Valter Torri:** Methodology, Data curation. **Cinzia Monti:** Investigation, Visualization. **Roberta Meroni:** Investigation, Visualization. **Giordano Domenico Beretta:** Supervision. **Massimo Castoldi:** Supervision. **Emilio Bombardieri:** Conceptualization, Methodology, Writing - review & editing, Funding acquisition.

Declaration of Competing Interest

The authors report no declarations of interest.

Acknowledgements

The Authors are grateful to all Colleagues, Nurses, Technologists, Volunteers and Administrative staff of Humanitas Gavazzeni who worked very hard assisting COVID-19 patients in a dramatic period of emergency and gave a generous personal and professional support. **We also thank Ray Hill**, an independent medical writer, who provided English-language editing and journal styling prior to submission on behalf of Health Publishing & Services Srl.

Appendix A. Supplementary data

Supplementary material related to this article can be found, in the online version, at doi:<https://doi.org/10.1016/j.ejrad.2021.109612>.

References

- [1] World Health Organization, WHO Coronavirus Disease (COVID-19) Dashboard, Available from: <https://covid19.who.int/> (Accessed 1 January 2021), 2021.
- [2] Johns Hopkins University (JHU), Coronavirus COVID-19 Global Cases by the Center for Systems Science and Engineering (CSSE), Available from: <https://coronavirus.jhu.edu/map.html> (Accessed 1 June 2020), 2020.
- [3] D. Baud, X. Qi, K. Nielsen-Saines, D. Musso, L. Pomar, G. Favre, Real estimates of mortality following COVID-19 infection, *Lancet Infect. Dis.* 20 (7) (2020) 773.
- [4] F. Zhou, T. Yu, R. Du, G. Fan, Y. Liu, Z. Liu, J. Xiang, Y. Wang, B. Song, X. Gu, L. Guan, Y. Wei, H. Li, X. Wu, J. Xu, S. Tu, Y. Zhang, H. Chen, B. Cao, Clinical course and risk factors for mortality of adult inpatients with COVID-19 in Wuhan, China: a retrospective cohort study, *Lancet* 395 (10229) (2020) 1054–1062.
- [5] Z. Wang, B. Yang, Q. Li, L. Wen, R. Zhang, Clinical features of 69 cases with coronavirus disease 2019 in Wuhan, China, *Clin. Infect. Dis.* 71 (15) (2020) 769–777.
- [6] Q. Ruan, K. Yang, W. Wang, L. Jiang, J. Song, Clinical predictors of mortality due to COVID-19 based on an analysis of data of 150 patients from Wuhan, China, *Intensive Care Med.* 46 (5) (2020) 846–848.
- [7] Y. Shi, X. Yu, H. Zhao, H. Wang, R. Zhao, J. Sheng, Host susceptibility to severe COVID-19 and establishment of a host risk score: findings of 487 cases outside Wuhan, *Crit. Care* 24 (1) (2020) 108.
- [8] A. Bernheim, X. Mei, M. Huang, Y. Yang, Z.A. Fayad, N. Zhang, K. Diao, B. Lin, X. Zhu, K. Li, S. Li, H. Shan, A. Jacobi, M. Chung, Chest CT findings in coronavirus disease-19 (COVID-19): relationship to duration of infection, *Radiology* 295 (3) (2020) 200463.
- [9] D.M. Hansell, A.A. Bankier, H. MacMahon, T.C. McLoud, N.L. Müller, J. Remy, Fleischner Society: Glossary of terms for thoracic imaging, *Radiology* 246 (3) (2008) 697–722.
- [10] G.D. Rubin, C.J. Ryerson, L.B. Haramati, N. Sverzellati, J.P. Kanne, S. Raouf, N. W. Schluger, A. Volpi, J.J. Yim, I.B.K. Martin, D.J. Anderson, C. Kong, T. Altes, A. Bush, S.R. Desai, J. Goldin, J.M. Goo, M. Humbert, Y. Inoue, H.U. Kauczor, F. Luo, P.J. Mazzone, M. Prokop, M. Remy-Jardin, L. Richeldi, C.M. Schaefer-Prokop, N. Tomiyama, A.U. Wells, A.N. Leung, The role of chest imaging in patient management during the COVID-19 pandemic: a multinational consensus statement from the Fleischner Society, *Chest* 158 (1) (2020) 106–116.
- [11] American College of Radiology (ACR), ACR Recommendations for the Use of Chest Radiography and Computed Tomography (CT) for Suspected COVID-19 Infection, Available from: <https://www.acr.org/Advocacy-and-Economics/ACR-Position%20Statements/Recommendations-for-Chest-Radiography-and-CT-for-Suspected-COVID19-Infection> (Accessed 1 June 2020), 2020.
- [12] S. Simpson, F.U. Kay, S. Abbara, S. Bhalla, J.H. Chung, M. Chung, T.S. Henry, J. P. Kanne, S. Kligerman, J.P. Ko, H. Litt, Radiological Society of North America Expert Consensus Statement on reporting chest CT findings related to COVID-19. Endorsed by the Society of Thoracic Radiology, the American College of Radiology, and RSNA – Secondary Publication, *J. Thorac. Imaging* 35 (4) (2020) 219–227.
- [13] M. Lang, A. Som, D.P. Mendoza, E.J. Flores, M.D. Li, J.O. Shepard, B.P. Little, Detection of unsuspected coronavirus disease 2019 cases by computed tomography and retrospective implementation of the Radiological Society of North America/Society of Thoracic Radiology/American College of Radiology Consensus Guidelines, *J. Thorac. Imaging* 35 (6) (2020) 346–353.

- [14] E.A. Akl, I. Blazic, S. Yaacoub, G. Frija, R. Chou, J.A. Appiah, M. Fatehi, N. Flor, E. Hitti, H. Jafri, Use of chest imaging in the diagnosis and management of COVID-19: a WHO rapid advice guide, *Radiology* 298 (2021) E63–E69.
- [15] O. Goletti, C. Nessi, A. Testa, G. Albano, V. Torri, G.D. Beretta, M. Castoldi, E. Bombardieri, Factors affecting mortality in 1022 COVID-19 patients referred to an emergency department in Bergamo during the peak of the pandemic, *SN Compr. Clin. Med.* (2020) 1–6.
- [16] V. Ojha, A. Mani, N.N. Pandey, S. Sharma, S. Kumar, CT in coronavirus disease 2019 (COVID-19): a systematic review of chest CT findings in 4410 adult patients, *Eur. Radiol.* 30 (11) (2020) 6129–6138.
- [17] H.J. Koo, S.H. Choi, H. Sung, J. Choe, K.H. Do, *RadioGraphics Update: Radiographic and CT features of viral pneumonia*, *Radiographics* 40 (4) (2020) E8–E15.
- [18] X. Xu, C. Yu, J. Qu, L. Zhang, S. Jiang, D. Huang, B. Chen, Z. Zhang, W. Guan, Z. Ling, R. Jiang, T. Hu, Y. Ding, L. Lin, Q. Gan, L. Luo, X. Tang, J. Liu, Imaging and clinical features of patients with 2019 novel coronavirus SARS-CoV-2, *Eur. J. Nucl. Med. Mol. Imaging* 47 (5) (2020) 1275–1280.
- [19] W. Zhao, Z. Zhong, X. Xie, Q. Yu, J. Liu, Relation between chest CT findings and clinical conditions of coronavirus disease (COVID-19) pneumonia: a multicenter study, *Am. J. Roentgenol.* 214 (5) (2020) 1072–1077.
- [20] K. Li, J. Wu, F. Wu, D. Guo, L. Chen, Z. Fang, C. Li, The clinical and chest CT features associated with severe and critical COVID-19 pneumonia, *Invest. Radiol.* 55 (6) (2020) 327–331.
- [21] M. Yuan, W. Yin, Z. Tao, W. Tan, Y. Hu, Association of radiologic findings with mortality of patients infected with 2019 novel coronavirus in Wuhan, China, *PLoS One* 15 (3) (2020), e0230548.
- [22] S.M.H. Tabatabaei, H. Talari, F. Moghaddas, H. Rajebi, CT features and short-term prognosis of COVID-19 pneumonia: a single-center study from Kashan, Iran, *Radiol. Cardiothoracic Imaging* 2 (2) (2020), e200130.
- [23] P. Lyu, X. Liu, R. Zhang, L. Shi, J. Gao, The performance of chest CT in evaluating the clinical severity of COVID-19 pneumonia: identifying critical cases based on CT characteristics, *Invest. Radiol.* 55 (7) (2020) 412–421.
- [24] G. Durhan, S. Ardali Duzgun, F. Basaran Demirkazik, I. Irmak, I. Idilman, M. Gulsun Akpınar, E. Akpınar, S. Ocal, G. Telli, A. Topeli, O.M. Ariyurek, Visual and software-based quantitative chest CT assessment of COVID-19: correlation with clinical findings, *Diagn. Interv. Radiol.* 26 (6) (2020) 557–564.
- [25] D. Caruso, M. Polici, M. Zerunian, F. Pucciarelli, T. Polidori, G. Guido, C. Rucci, B. Bracci, E. Muscogiuri, C. De Dominicis, A. Laghi, Quantitative chest CT analysis in discriminating COVID-19 from non-COVID-19 patients, *Radiol. Med.* 126 (2) (2021) 243–249.
- [26] D. Ippolito, M. Ragusi, D. Gandola, C. Maino, A. Pecorelli, S. Terrani, M. Peroni, T. Giandola, M. Porta, C. Talei Franzesi, S. Sironi, Computed tomography semi-automated lung volume quantification in SARS-CoV-2-related pneumonia, *Eur. Radiol.* 30 (2020) 1–11.
- [27] A. Leonardi, R. Scipione, G. Alfieri, R. Petrillo, M. Dolciami, F. Ciccarelli, S. Perotti, G. Cartocci, A. Scala, C. Imperiale, F. Iafrate, M. Francone, C. Catalano, P. Ricci, Role of computed tomography in predicting critical disease in patients with covid-19 pneumonia: a retrospective study using a semiautomatic quantitative method, *Eur. J. Radiol.* 130 (2020), 109202.
- [28] I. Ozsahin, B. Sekeroglu, M.S. Musa, M.T. Mustapha, D. Uzun Ozsahin, Review on diagnosis of COVID-19 from chest CT images using artificial intelligence, *Comput. Math. Methods Med.* 2020 (2020).
- [29] S.A. Harmon, T.H. Sanford, S. Xu, E.B. Turkbey, H. Roth, Z. Xu, D. Yang, A. Myronenko, V. Anderson, A. Amalou, M. Blain, M. Kassin, D. Long, N. Varble, S. M. Walker, U. Bagci, A.M. Ierardi, E. Stellato, G.G. Plensich, G. Franceschelli, C. Girlando, G. Irmici, D. Labella, D. Hammoud, A. Malayeri, E. Jones, R. M. Summers, P.L. Choyke, D. Xu, M. Flores, K. Tamura, H. Obinata, H. Mori, F. Patella, M. Cariati, G. Carrafiello, P. An, B.J. Wood, B. Turkbey, Artificial intelligence for the detection of COVID-19 pneumonia on chest CT using multinational datasets, *Nat. Commun.* 11 (1) (2020) 4080.
- [30] R.M. Summers, Artificial Intelligence of COVID-19 imaging: a hammer in search of a nail, *Radiology* (2020), 204226.
- [31] D. Toussie, N. Voutsinas, M. Finkelstein, M.A. Cedillo, S. Manna, S.Z. Maron, A. Jacobi, M. Chung, A. Bernheim, C. Eber, J. Concepcion, Z. Fayad, Y.S. Gupta, Clinical and chest radiography features determine patient outcomes in young and middle age adults with COVID-19, *Radiology* (2020) 201754.
- [32] A.J. Rodriguez-Morales, J.A. Cardona-Ospina, E. Gutierrez-Ocampo, R. Villamizar-Pena, Y. Holguin-Rivera, J.P. Escalera-Antezana, L.E. Alvarado-Arnez, D.K. Bonilla-Aldana, C. Franco-Paredes, A.F. Henao-Martinez, A. Paniz-Mondolfi, G.J. Lagos-Grisales, E. Ramirez-Vallejo, J.A. Suarez, L.I. Zambrano, W.E. Villamil-Gomez, G. J. Balbin-Ramon, A.A. Rabaan, H. Harapan, K. Dhama, H. Nishiura, H. Kataoka, T. Ahmad, R. Sah, Latin American Network of Coronavirus Disease 2019-COVID-19 Research (LANCOVID-19), Clinical, laboratory and imaging features of COVID-19: a systematic review and meta-analysis, *Travel Med. Infect. Dis.* 34 (2020), 101623.
- [33] D. Colombi, F.C. Bodini, M. Petrini, G. Maffi, N. Morelli, G. Milanese, M. Silva, N. Sverzellati, E. Michieletti, Well-aerated lung on admitting chest CT to predict adverse outcome in COVID-19 pneumonia, *Radiology* 296 (2) (2020) E86–E96.
- [34] X. Chen, Y. Tang, Y. Mo, S. Li, D. Lin, Z. Yang, Z. Yang, H. Sun, J. Qiu, Y. Liao, J. Xiao, X. Chen, X. Wu, R. Wu, Z. Dai, A diagnostic model for coronavirus disease 2019 (COVID-19) based on radiological semantic and clinical features: a multicenter study, *Eur. Radiol.* 30 (9) (2020) 4893–4902.
- [35] E. Guillo, I. Bedmar Gomez, S. Dangeard, S. Bennani, I. Saab, M. Tordjman, L. Jilet, G. Chassagnon, M.P. Revel, COVID-19 pneumonia: diagnostic and prognostic role of CT based on a retrospective analysis of 214 consecutive patients from Paris, France, *Eur. J. Radiol.* 131 (2020), 109209.
- [36] S. Meiler, J. Schaible, F. Poschenrieder, G. Scharf, F. Zeman, J. Rennert, B. Pregler, H. Kleine, C. Stroszczyński, N. Zorger, O.W. Hamer, Can CT performed in the early disease phase predict outcome of patients with COVID 19 pneumonia? Analysis of a cohort of 64 patients from Germany, *Eur. J. Radiol.* 131 (2020), 109256.
- [37] A. Borghesi, A. Zigliani, R. Masciullo, S. Golemi, P. Maculotti, D. Farina, R. Maroldi, Radiographic severity index in COVID-19 pneumonia: relationship to age and sex in 783 Italian patients, *Radiol. Med.* 125 (5) (2020) 461–464.
- [38] Z. Shahid, R. Kalayanamitra, B. McClafferty, D. Kepko, D. Ramgobin, R. Patel, C. S. Aggarwal, R. Vunnam, N. Sahu, D. Bhatt, K. Jones, R. Golamari, R. Jain, COVID-19 and older adults: what we know, *J. Am. Geriatr. Soc.* 68 (5) (2020) 926–929.
- [39] W.J. Guan, Z.Y. Ni, Y. Hu, W.H. Liang, C.Q. Ou, J.X. He, L. Liu, H. Shan, C.L. Lei, D. S.C. Hui, B. Du, L.J. Li, G. Zeng, K.Y. Yuen, R.C. Chen, C.L. Tang, T. Wang, P. Y. Chen, J. Xiang, S.Y. Li, J.L. Wang, Z.J. Liang, Y.X. Peng, L. Wei, Y. Liu, Y.H. Hu, P. Peng, J.M. Wang, J.Y. Liu, Z. Chen, G. Li, Z.J. Zheng, S.Q. Qiu, J. Luo, C.J. Ye, S. Y. Zhu, N.S. Zhong, C. China Medical Treatment Expert Group for, Clinical characteristics of Coronavirus Disease 2019 in China, *N. Engl. J. Med.* 382 (18) (2020) 1708–1720.
- [40] Y. Liu, Y. Yang, C. Zhang, F. Huang, F. Wang, J. Yuan, Z. Wang, J. Li, J. Li, C. Feng, Z. Zhang, L. Wang, L. Peng, L. Chen, Y. Qin, D. Zhao, S. Tan, L. Yin, J. Xu, C. Zhou, C. Jiang, L. Liu, Clinical and biochemical indexes from 2019-nCoV infected patients linked to viral loads and lung injury, *Sci. China Life Sci.* 63 (3) (2020) 364–374.
- [41] C. Huang, Y. Wang, X. Li, L. Ren, J. Zhao, Y. Hu, L. Zhang, G. Fan, J. Xu, X. Gu, Z. Cheng, T. Yu, J. Xia, Y. Wei, W. Wu, X. Xie, W. Yin, H. Li, M. Liu, Y. Xiao, H. Gao, L. Guo, J. Xie, G. Wang, R. Jiang, Z. Gao, Q. Jin, J. Wang, B. Cao, Clinical features of patients infected with 2019 novel coronavirus in Wuhan, China, *Lancet* 395 (10223) (2020) 497–506.
- [42] W.J. Guan, W.H. Liang, Y. Zhao, H.R. Liang, Z.S. Chen, Y.M. Li, X.Q. Liu, R.C. Chen, C.L. Tang, T. Wang, C.Q. Ou, L. Li, P.Y. Chen, L. Sang, W. Wang, J.F. Li, C.C. Li, L. M. Ou, B. Cheng, S. Xiong, Z.Y. Ni, J. Xiang, Y. Hu, L. Liu, H. Shan, C.L. Lei, Y. X. Peng, L. Wei, Y. Liu, Y.H. Hu, P. Peng, J.M. Wang, J.Y. Liu, Z. Chen, G. Li, Z. J. Zheng, S.Q. Qiu, J. Luo, C.J. Ye, S.Y. Zhu, L.L. Cheng, F. Ye, S.Y. Li, J.P. Zheng, N.F. Zhang, N.S. Zhong, J.X. He, China Medical Treatment Expert Group for COVID-19, Comorbidity and its impact on 1590 patients with COVID-19 in China: a nationwide analysis, *Eur. Respir. J.* 55 (5) (2020).
- [43] B. Li, J. Yang, F. Zhao, L. Zhi, X. Wang, L. Liu, Z. Bi, Y. Zhao, Prevalence and impact of cardiovascular metabolic diseases on COVID-19 in China, *Clin. Res. Cardiol.* 109 (5) (2020) 531–538.
- [44] V. Jain, J.M. Yuan, Predictive symptoms and comorbidities for severe COVID-19 and intensive care unit admission: a systematic review and meta-analysis, *Int. J. Public Health* 65 (5) (2020) 533–546.
- [45] C.I. Vardavas, K. Nikitara, COVID-19 and smoking: A systematic review of the evidence, *Tob. Induc. Dis.* 18 (2020) 20.
- [46] J. Yang, Y. Zheng, X. Gou, K. Pu, Z. Chen, Q. Guo, R. Ji, H. Wang, Y. Wang, Y. Zhou, Prevalence of comorbidities in the novel Wuhan coronavirus (COVID-19) infection: a systematic review and meta-analysis, *Int. J. Infect. Dis.* 94 (5) (2020) 91–95.
- [47] Y. Nguyen, F. Corre, V. Honsel, S. Curac, V. Zarrouk, C.P. Burtz, E. Weiss, J. D. Moyer, T. Gauss, J. Gregory, F. Bert, C. Trichet, K. Peoc'h, V. Vilgrain, V. Rebours, B. Fantin, A. Galy, A nomogram to predict the risk of unfavourable outcome in COVID-19: a retrospective cohort of 279 hospitalized patients in Paris area, *Ann. Med.* 52 (7) (2020) 367–375.
- [48] Y. Yu, X. Wang, M. Li, L. Gu, Z. Xie, W. Gu, F. Xu, Y. Bao, R. Liu, S. Hu, M. Hu, C. Hu, Nomogram to identify severe coronavirus disease 2019 (COVID-19) based on initial clinical and CT characteristics: a multi-center study, *BMC Med. Imaging* 20 (1) (2020) 111.